International Journal of Advanced Technology and Engineering Exploration, Vol 11(114)
ISSN (Print): 2394-5443 ISSN (Online): 2394-7454
http://dx.doi.org/10.19101/IJATEE.2023.10102385

Research Article

Optimizing energy production: superiority of feasible solution-moth flame optimization in IEEE 57-bus systems for optimal power flow

Mohammad Khurshed Alam[1, 2*], Mohd Herwan Sulaiman[1], Md. Shaoran Sayem[2], Asma Ferdowsi[3], Md. Foysal[2] and Md. Mahfuzur Akter Ringku[2]
Faculty of Electrical & Electronics Engineering Technology, Universiti Malaysia Pahang Al-Sultan Abdullah (UMPSA), 26600 Pekan, Pahang, Malaysia[1]
Department of Electrical & Electronics Engineering, American International University-Bangladesh, Dhaka-1229, Bangladesh[2]
Pharmacology Department, Sir Salimullah Medical College Hospital, Mitford Rd, Dhaka 1206.Bangladesh[3]

Received: 08-October-2023; Revised: 26-May-2024; Accepted: 28-May-2024

Abstract
Optimal Power Flow (OPF) presents a formidable challenge in power systems, characterized by non-convex and non-linear optimization constraints. Significant attention has been dedicated to addressing this issue, particularly in optimizing control variables, given their crucial role in achieving system objectives while ensuring stability. Consequently, OPF remains a focal point in power systems engineering. This study utilizes the superiority of feasible solution-moth flame optimization (SF-MFO) algorithm to tackle five key objectives in the OPF problem. These objectives include minimizing power generation costs, reducing power loss, emissions, voltage deviation, and optimizing both cost and emissions simultaneously across various power generation sources, such as thermal and stochastic wind-solar-small hydro. Evaluation of SF-MFO's performance in handling the OPF problem involves utilizing IEEE 57-bus systems integrated with stochastic wind-solar-small hydro power generators. Statistical analyses demonstrate SF-MFO's consistent superiority over alternative metaheuristic algorithms across all simulation scenarios. For instance, in power generation cost and emissions, the IEEE 57-bus systems achieve a rate of 28129.41033 $/hr, representing a 1.02% cost saving per hour compared to the worst results obtained from other algorithms. The study indicates SF-MFO's efficacy in navigating complex search spaces while maintaining feasibility, offering a promising approach to address energy optimization challenges.

Keywords
Emission control, Forbidden operating zones, Grey wolf optimization (GWO), SF-MFO.

1.Introduction
Optimal power flow (OPF) stands as a cornerstone problem in power systems engineering, aiming to minimize generation costs while adhering to various operational constraints such as power flow equations, transmission limits, and environmental regulations. Its significance lies in its crucial role in enhancing the efficiency, reliability, and sustainability of electric power networks, making it an essential tool for the efficient management and strategic planning of power grid systems [1]. As energy prices soar and fossil fuel resources gradually deplete, the urgency for enhanced energy efficiency and more intelligent energy management approaches becomes increasingly evident.

OPF is vital for operators in the planning and operational stages of modern power systems, with the primary aim being to identify the most efficient operating state that ensures economical operation while meeting diverse requirements and upholding equal standards. Mathematical techniques such as split Bregman method [2], sequential quadratic programming (SQP) [3], simplex-based sequential linear programming (SLP) [4], linear programming (LP) [5], nonlinear programming (NLP) [6], quadratic programming (QP) [7], integer programming (IP) [8], Newton methods (NM) [9], decomposition method (DM) [10], and fast successive linear programming algorithm (FSLPA) [11]. Evolutionary algorithms (EA) have been employed to tackle the complexities of OPF optimization. While traditional methods often derive

*Author for correspondence

effective solutions from continuous differentiable and convex functions, challenges persist due to the non-convex and non-smooth nature of certain aspects of OPF, such as optimal reactive power dispatch (ORPD) [12] and economic dispatch (ED).

Despite significant advancements in OPF optimization techniques, challenges remain that hinder the efficient resolution of the problem. Computational inefficiency, scalability issues, and difficulty handling diverse constraints have been identified as significant hurdles. Traditional optimization algorithms may suffer from premature convergence and poor performance in handling non-convex and discontinuous objective functions typical in OPF formulations. Although EA like genetic algorithm(GA) [13] , evolutionary programming (EP) [14], particle swarm optimization (PSO) [15], modified shuffle frog leaping algorithm (MSLFA) [16], success-history based adaptive differential evolution (SHADE) [17], gravitational search algorithm (GSA) [18], Grey wolf optimization (GWO) [19], and moth flame optimization (MFO) [20] offer promising solutions, challenges such as trapping in local optima and slow convergence to global optima persist. Furthermore, the selection and tuning of parameters in EA, such as the scaling factor (F) and crossover rate (CR), pose additional challenges in achieving optimal performance. The need for innovative approaches to address these challenges is evident, emphasizing the necessity for further research and development in the field of OPF optimization.

Motivated by the significant challenges inherent in solving OPF problems using traditional optimization techniques, our work aims to explore the potential of the superiority of feasible solution-moth flame optimization (SF-MFO) algorithm in addressing these challenges. The nonlinearity, high dimensionality, and complexity of power system models pose substantial obstacles to efficient optimization, necessitating innovative and efficient approaches. SF-MFO, as an extension of the MFO algorithm, is specifically designed to prioritize feasible solutions, aligning well with the constraints inherent in OPF problems. By integrating the principles of MFO with a focus on feasibility, SF-MFO offers a robust and reliable framework for tackling OPF challenges effectively. Our motivation stems from the urgent need to enhance the efficiency, reliability, and sustainability of electric power networks, especially in the face of soaring energy prices and the gradual depletion of fossil fuel resources.

The objectives of this study are threefold. Firstly, the effectiveness of SF-MFO in minimizing generation costs while satisfying operational constraints in power systems is evaluated. Secondly, the performance of SF-MFO is compared with other state-of-the-art optimization algorithms commonly used for solving OPF problems, providing insights into its relative efficacy and potential advantages. Lastly, the impact of different problem formulations and constraints on the performance of SF-MFO is analyzed, shedding light on its adaptability and robustness across varying scenarios.

The primary contributions of this paper include the introduction of SF-MFO as a novel optimization approach for solving OPF problems, with a specific emphasis on feasibility as a key objective. Additionally, a comprehensive empirical study was conducted to assess the performance of SF-MFO in comparison to other optimization algorithms, providing valuable insights into its strengths and limitations. Furthermore, insights into addressing various OPF challenges are offered, and opportunities for further research and improvement are identified, thereby contributing to the advancement of efficient and effective solutions for power systems optimization.

The structure of this paper is as follows: In section 2, a comprehensive literature review of OPF and its associated optimization techniques is provided, offering a contextual background for the study. Section 3 details the methodology employed, including the formulation of the OPF problem and the intricate implementation details of the SF-MFO algorithm. Subsequently, section 4 outlines the experimental setup utilized, presenting results and their subsequent analysis. In section 5, a detailed discussion of the findings obtained from the study is presented, exploring their implications and significance within the broader context of power systems optimization. Finally, in section 6, conclusions are drawn from the research, and potential directions for future investigations in this field are outlined, encapsulating the essence of the contributions and paving the way for further advancements.

2.Literature review

The traditional methods of setting local limits on generating power have encountered significant challenges when compared to the OPF method, as highlighted in the introduction. Traditional approaches often rely on static constraints and

localized adjustments, which can be inadequate for modern, dynamic power systems. OPF offers a more sophisticated approach to managing generator restrictions, utilizing techniques such as voltage critical analysis [21], clamp mechanisms [22], punishment function logic [23], and higher voltage limits [24] to optimize performance. These techniques enable dynamic adjustments and fine-tuning of system parameters, enhancing overall efficiency and stability. However, concerns persist regarding the complexity of OPF [25] and its differentiation from standard power flows [26], posing usability issues, especially for new users. The mathematical and computational intricacies of OPF algorithms require specialized knowledge and significant computational resources, which can be barriers to entry. Nevertheless, advancements in OPF planning tools aim to address these challenges by offering comprehensive functionalities, including preventive and corrective tuning [27], adaptable system responses [28], and efficient problem-solving capabilities [29]. These tools are designed to simplify the user experience, making OPF more accessible and effective. Research indicates that OPF can significantly enhance system reliability and efficiency, particularly in deregulated markets, by optimizing pricing strategies and ensuring stability amidst real-time processing demands. Furthermore, OPF's role in emergency response and risk mitigation underscores its critical importance in maintaining operational resilience. Despite its advantages, challenges such as parameter sensitivity and computational complexity necessitate ongoing refinement of OPF methodologies. Ensuring user accessibility through improved interface design and training remains essential for broader adoption. In conclusion, while OPF presents a complex but superior alternative to traditional methods, continuous advancements in tools and training are crucial for maximizing its potential in modern power systems.

Research outcomes demonstrate the significant potential of OPF in addressing complex energy market [30] challenges, particularly in deregulated environments [31]. OPF's advanced capabilities allow it to effectively navigate market dynamics by optimizing the dispatch of generation resources to minimize costs and maximize efficiency [32]. This optimization extends to pricing strategies, where OPF can dynamically adjust to market conditions, ensuring competitive and fair pricing. Studies have shown that OPF enhances system stability by balancing supply and demand in real-time, thus mitigating the risks associated with fluctuations in generation and load. The ability to process real-time data and adjust operational parameters accordingly makes OPF indispensable in environments with multiple market rivals and variable demand [33]. Furthermore, OPF's role in emergency response coordination is critical; it can quickly reconfigure the power system to maintain stability during unexpected events, thereby minimizing outages and maintaining service reliability. Research highlights OPF's effectiveness in risk mitigation, particularly in scenarios involving natural disasters or sudden system failures, where rapid response is crucial to prevent widespread disruption. Additionally, the implementation of OPF in preventive and corrective control strategies has been shown to improve the resilience of power systems by proactively addressing potential issues before they escalate. Despite these advantages, ongoing research emphasizes the need for continuous improvement in OPF algorithms to address challenges such as computational complexity and integration with renewable energy sources. Advances in machine learning and heuristic methods are being explored to enhance the efficiency and scalability of OPF solutions [34]. Overall, the comprehensive literature underscores OPF's pivotal role in modern energy management, highlighting its potential to revolutionize how power systems operate and respond to both market and operational challenges.

The advantages of OPF are manifold, ranging from its ability to optimize resource allocation and enhance system efficiency to its versatility in accommodating diverse operational requirements. OPF's sophisticated algorithms enable precise adjustments in power generation and distribution, ensuring that resources are used optimally to meet demand while minimizing costs. This optimization is crucial in maintaining system efficiency and reliability, particularly in complex power networks. Literature indicates that OPF allows users to make informed decisions by providing detailed insights into system performance and potential improvements, thereby facilitating strategic planning and operational adjustments. The adaptability of OPF to changing environmental and market conditions is another significant benefit. For instance, OPF can integrate renewable energy sources more effectively, adjusting for variability in wind or solar generation. Furthermore, the integration of conventional optimization techniques with metaheuristic methodologies, such as GA and PSO, enhances OPF's robustness and performance across various scenarios. These metaheuristic methods are

particularly effective in solving non-linear, multi-objective optimization problems commonly found in power systems, providing flexible and scalable solutions. Research highlights that the scalability of OPF is essential for its application in both small-scale distributed generation systems and large-scale grid operations. Additionally, advanced OPF models have been shown to improve voltage stability and reduce transmission losses, further enhancing overall system performance. Despite these strengths, continuous advancements in OPF techniques are necessary to address emerging challenges, such as integrating distributed energy resources and enhancing real-time operation capabilities. Overall, the comprehensive analysis of relevant literature underscores OPF's critical role in modern power system management, demonstrating its potential to significantly improve efficiency, adaptability, and reliability in an evolving energy landscape.

Despite its strengths, OPF is not without limitations. Challenges such as parameter sensitivity, computational complexity, and scalability issues may hinder its widespread adoption and effectiveness in certain contexts. Parameter sensitivity refers to the significant impact that initial conditions and parameter settings can have on OPF outcomes, potentially leading to variability and unpredictability in results. This sensitivity necessitates precise calibration and robust validation to ensure reliable performance. Computational complexity is another major hurdle; solving OPF problems involves intricate mathematical formulations and extensive computational resources, particularly for large-scale power systems with numerous variables and constraints. This complexity can make real-time application difficult, limiting OPF's utility in fast-changing operational environments. Scalability issues also pose a challenge, as expanding OPF methodologies to accommodate larger or more complex systems often results in increased computation times and difficulties in maintaining optimal performance. Furthermore, the evolving nature of energy markets and regulatory frameworks necessitates ongoing refinement and adaptation of OPF methodologies. As markets become more deregulated [35] and competitive, OPF must adapt to new pricing mechanisms, market rules, and trading strategies to remain effective. Regulatory changes can alter operational constraints and objectives, requiring continuous updates to OPF models and approaches to stay compliant and functional. Ensuring accessibility and usability for diverse user groups remains a significant challenge. Advanced OPF tools often require specialized knowledge and technical expertise, which can be a barrier to widespread adoption among utility operators and engineers who may lack such training. To address this, there is a need for improved user interface design and comprehensive training initiatives that make OPF tools more intuitive and user-friendly [36]. Literature suggests that integrating OPF with modern technologies like machine learning and artificial intelligence can mitigate some of these limitations by enhancing adaptability, predictive capabilities, and overall efficiency. These technologies can help OPF respond more effectively to dynamic system conditions and market fluctuations. Additionally, research into decentralized and distributed OPF approaches is promising, as these methods can improve scalability and reduce computational burdens by leveraging parallel processing and localized optimization techniques. By distributing the computational load and optimizing smaller sections of the grid independently, these approaches can enhance the overall performance and applicability of OPF. In conclusion, while OPF is a powerful tool for optimizing power systems, addressing its limitations through ongoing research and technological integration is crucial. Enhancing computational efficiency, adaptability, and user accessibility will ensure that OPF continues to play a vital role in the efficient and reliable operation of modern power grids.

3.Methods

This section explores the complete methodology. The mathematical interpretation is arranged with several phases of operations. The optimization parameters and criteria are also discussed here elaborately. At first, the phase 1 ORPD issue is described as shown in Equation 1:

$$\text{Minimize } f=(x,u); \quad s.t.\begin{cases} g(x,u)=0 \\ h(x,u)=0 \end{cases} \quad (1)$$

where $\boldsymbol{x}$ is the vector of dependent variables, $\boldsymbol{u}$ is the vector of control variables, $f(x, u)$ is the objective function, $g(x, u)=0$, as well as $h(x, u)=0$ are similarity and no similarity.

Phase 2 discusses the ED issue and which goal function of the ED problem should be kept to a minimum. The objective function is as follows: F_i (P_{Gi}) is the operating fuel cost for N number of generating units, and min (F_r) is the total fuel cost (Equation 2).

$$\min\ (F_r)=\min \sum_{i=1}^{N} F_i(P_{Gi}) \quad (2)$$

3.1Generation cost minimization

The generator cost curve is represented by quadratic functions [37], and the total fuel cost $F(G_i)$ in $/h) can be expressed as (Equation 3):

$$F_i(P_{Gi}) = \sum_{i=1}^{N} a_i + b_i P_{Gi} + c_i P_{Gi} \quad (3)$$

where N is the aggregate of alternators, a_i, b_i, and c_i are each alternator's price degree, and P_G is a direction representing the original energy achievement of the alternators. The energy unit uses several stopcocks to regulate the return energy of all alternators. In a turbine, each condensation entry gate begins to open, causing the stopcocks to point to fill up the result, which ripples the price curve, as seen in *Figure 1*. To mitigate this consequence in the profitable load transmitted problem the oscillatory consequence into the equilateral price justification as follows Equation 4:

$$F_T = \left(\sum_{i=1}^{n} F_i(P_{Gi}) \right) = \left(\sum_{i=1}^{n} a_i P_{Gi}^2 + c_i + \left| e_i \times \sin(f_i \times (P_{Gi}^{\min} - P_{Gi})) \right| \right) \quad (4)$$

To which the coefficients e_i and f_i of the i^{th} alternator are replaced with stopcocks and point charge. When integrating sustainable power origin, namely solar and wind, into the grid, their prime is to consider that these sources have particular characteristics, such as uncertainty and intermittency. Typically, private entities that own wind farms and solar photovoltaic (PV) cell systems enter a buy harmony of planned energy, including independent system operators (ISO). In this way, the overall price of the particular energy plant is broken down into its parts: straight price, secondary price, and forfeit price. The following is a breakdown of the direct expenses of using blow and cosmic PV generators Equation 5 and 6:

$$Cost_{wj}(P_{wGi}) = g_{WGj} P_{WGJ} \quad (5)$$

$$Cost_{s,k}(P_{SGJ}) = g_{SG,k} P_{SG,k} \quad (6)$$

where g_{WGj} is the straight price portion for the j^{th} blow energy factory and $g_{SG,k}$ is the immediate price portion for the k^{th} cosmic power factory. Power output from wind farm j ($P_{WG,j}$) and solar farm k ($P_{SG,k}$) are on the schedule.

$$CostSHG(PSHG) = Cost(PSG + PHG) = gSGPSg + gHGPHG \quad (7)$$

Where pumped-storage hydro generators (PSHG) indicate the planned achievement of the PV+PSG+SHU energy station, PSG is the immediate price portion for PV, and gHG is the immediate price portion for solar hydro unit (SHU). It is important to note that the amount of arranged energy production accepted by ISO is predetermined; furthermore, an already stated amount of electricity will be delivered to the bus by combining cosmic PV and minor renewable sources. However, hydropower achievement fluctuates with the application rate of the stream (presume a stable governor head for run-of-stream supervision), and the factor is typically operated at full power because the magnitude, along with the volatility of the inconsiderable renewable, is negligible.

The energy generated by the breeze station or cosmic unit may be under the predicted amount. The system operator must maintain a spinning reserve in case of misjudgment of energy taken by an unknown source, which is necessary to maintain a constant supply to the customers. Reserve cost is described for sustainable power origin like a breeze and cosmic as "the cost of committing the reserve generating units to meet over-estimated values Equation 8."

$$Cost_{RWj}(P_{WGj} - P_{Wav,j}) = K_{RWj}(P_{WG,J} - P_{wav,j}) = K_{RW,j} \int_{0}^{P_{WG,j}} (P_{WG,j} - P_{W,j}) f_w(P_{W,j}) d_{pW,j}$$

$$Cost_{Rs,K}(P_{SG,k} - P_{S\,av,k}) = K_{Rs,K} * f_s(P_{Sav,k} < P_{SG,K}) * [P_{Sav,k} < P_{SG,K} - E(P_{Sav,k} < P_{SG,K})] \quad (8)$$

Thus, $K_{RW,j}$ is the secondary price portion of the j^{th} breeze energy unit, $P_{Wav,j}$ is the actual available power of the same plant, and $f_w(P_{W,j})$ is the wind power probability density function (PDF). However, $P_{Sav,k}$ represents the definitely attainable energy from the identical unit, $f_s(P_{S\,av,k}\ P_{SG,k})$ represents the chance of cosmic energy shortfall eventuality relative to the scheme energy ($P_{SG,k}$), and $E(P_{Sav,k}\ P_{SG,k})$ represents the prediction of cosmic PV energy below $P_{SG,k}$. Here is an expression for the reserve price that equates with overestimating cosmic PV and minor renewable sources together Equation 9:

$$Cost_{RSH}(P_{SHG} - P_{SHav}) = K_{RSH}(P_{SHG} - P_{Shav}) = K_{RSH} * f_{SH}(P_{Shav} < P_{SGH}) * [P_{SHG} < E(P_{Shav} < P_{SHG})] \quad (9)$$

where K_{RSH} is the combined system's cost coefficient, P_{Shav} is the plant's real available power, and f_{SH} (P_{SHav} P_{SHG}) is the probability that the plant's solar and micro hydropower is insufficient. The conjecture of cosmic PV and minor renewable sources below PSHG is denoted by E (P_{SHav}, P_{SHG}). The opposite of

overestimating power would be a circumstance in which real power delivered ensures greater than expected values, in which case the surplus power would be available. To address this issue, the forfeit cost associated with the excess aggregate of energy should be ensured, which for breeze and cosmic energy facilities can be written as follows Equation 10:

$$Cost_{PWj}\,(P_{Wav,J}-P_{WGj})=K_{PW,j}(P_{Wav,J}-P_{WGj})$$
$$=K_{PW,j}\int_{P_{WG,j}}^{Wr,J}(P_{W,j}-P_{WG,j})\,f_w(P_{W,j})d_{pw,j}$$
$$Cost_{PS,K}\,(P_{Sav,k}-P_{SG,k})=K_{PS,K}\,(P_{Sav,k}-P_{SG,k}) \quad (10)$$

thus $K_{PW,j}$ is the sanction price portion for breeze energy unit j, $P_{Wr,j}$ is the appraised achievement energy from the identical wind energy, $K_{PS,k}$ is the forfeit price portion for cosmic PV unit k, $f_s(P_{Sav,k} > P_{SG,k})$ is the expectation of cosmic energy surplus over the scheme energy ($P_{SG,k}$), and E($P_{Sav,k} > P_{SG,k}$) is the prediction of cosmic PV energy above $P_{SG,k}$.

3.2Transmission line minimization

Total distribution dropping F1 and potential function at delivery lines F2 [38] are the objective functions to be reduced, and they are written as follows Equation 11and 12.

$$F_1 = P_{loss}(x,u) = \sum_{L=1}^{Nl} P_{loss} \quad (11)$$
$$F_2 = VD(x,u) = \sum_{i=1}^{Nd} \left|V_i - V_i^{sp}\right| \quad (12)$$

Here, *Nls* = quantity of distribution buses; V_i = potential at delivery line i; N_d = quantity of delivery lines, where V_i is the potential at delivery line i, and the required value is ordinarily 1.0 p.u. The following are the power balances of load flow equality constraints Equation 13 and 14:

$$P_{Gi} - P_{Di} = V_i \sum_{jeNi} V_j (G_{ij}\cos\theta_{ij} + B_{ij}\sin\theta_{ij}) \quad (13)$$
$$Q_{Gi} - Q_{Di} = V_i \sum_{jeNi} V_j (B_{ij}\cos\theta_{ij} - G_{ij}\sin\theta_{ij}) \quad (14)$$

In contrast, operating constraints can be used to describe the inequality restrictions, described as Equation 15,

$$P_{Gi}^{\min} \le P_{Gi} \le P_{Gi}^{\max} \qquad i=1,\ldots,NG \quad (15)$$

Limits on the highest and lowest rate for both actual and phantom energy production, as well as for production line potential, are described as follows Equation 16 and 17:

$$Q_{Gi}^{\min} \le Q_{Gi} \le Q_{Gi}^{\max} \qquad i=1,\ldots,NG \quad (16)$$
$$V_{Gi}^{\min} \le V_{Gi} \le V_{Gi}^{\max} \qquad i=1,\ldots,NG \quad (17)$$

For some arbitrary number of generators, *NG*. Tap positions on a transformer have restricted each other by highest and lowest rate, as shown below Equation 18:

$$T_i^{\min} \le T_i \le T_i^{\max} \qquad i=1,\ldots,N_T \quad (18)$$

where N_T is the regulator. Phantom repayment (switch VARs) is confined by its restrictions as under Equation 19:

$$Q_{ci}^{\min} \le Q_{ci} \le Q_{ci}^{\max} \qquad i=1,\ldots,N_c \quad (19)$$

Thus, N_C is the total number of switch regulators.

3.3Maximum energy movement with the random breeze and cosmic energy

The best energy movement for classical systems using conventional (thermal) generators is an irregular multiplex issue with random restrictions. The problem becomes even more complicated when variable energy sources like solar and wind are included.

Table 1 displays the proposed explication for excellent energy circulation in the system, which involves a speculative breeze with cosmic energy and more traditional thermal power. Furthermore, *Table 2* provides information about the probability density functions (PDFs) for Weibull and lognormal distributions. The *Figure 1* depict solar irradiance and *Figure 2* represents actual power. The information in *Table 2* is mainly about the characteristics of pulse breeze power feeder measures at 11. The goal function factors in reserve costs exaggerate with the forfeit price since the variable sustainable energy origins are underestimated. Case studies' aims typically encompass emission factors as well. Breeze dispersion is represented using Weibull PDF, and the lognormal irradiance distribution is used to predict wind and PV power in *Figure 3*.

Environmentally hazardous gases are released into the atmosphere by thermal generators powered by fossil fuels. In optimization, some governments charge a "carbon tax" [39, 40] based on the total tonnage of carbon dioxide and other greenhouse gases released into the atmosphere. The effects of a fluctuating reserve, a restricted scheduling area [41], and associated penalty fees are analyzed. This research modifies the IEEE 57-feeder structure [42] to work along sustainable power origin breeze and cosmic.

While sustainable power origin does not possess generation costs, they affect generator scheduling. Researchers have combined the consignment of the levy with the objective events.

Table 1 The IEEE-57 feeder for consideration

Element	Number	Factor
Buses	30	[40]
Subdivide	41	[40]
Thermoelectric Turbines (TG1, TG2, TG3)	3	Feeders:1(sway),2 and 8
Breeze Turbines (WG1, WG2)	2	Feeders:5 and 11
PV Cosmic units (SPV)	1	Feeder:13
Constant tolerant	11	Scheme real energy for five alternators and potential on the feeder for every alternator feeder (6 Nos.)
Load Connected	-	285.4 MW, 127.2 MVAr
potential span in capacity Feeder	24	[0.96–1.06] p.u

Table 2 Breeze power feeder at 11

Standard function	Dissemination	Shortest cost Amount ($/WM)	Amount of conserve cost ($/MW)	Amount of penalty cost ($/MW)
50 MW	M=5, σ=0.6	g_{sG}=1.4	K_{rs}=2.1	K_{ps}=2.1

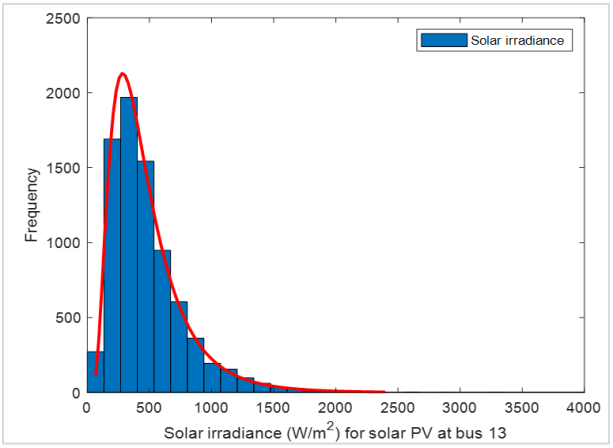

Figure 1 Solar PV at Bus 13.

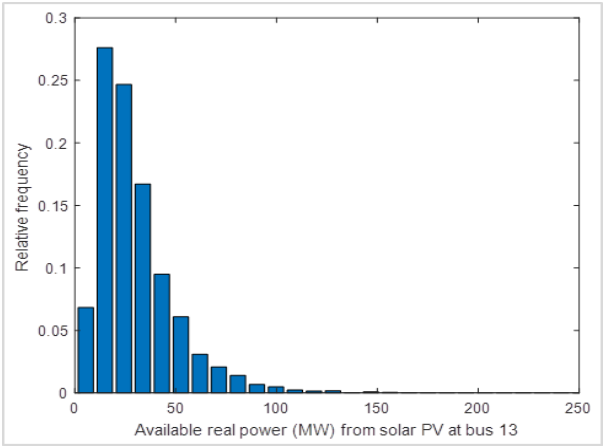

Figure 2 The actual amount of available power on bus 13

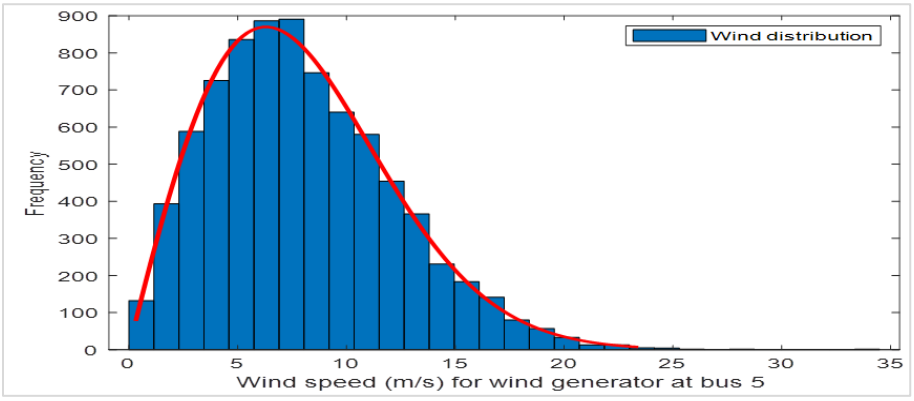

Figure 3 Wind speed for wind generator at bus 5

3.4An appropriate multi-goal evolutionary

The algorithm can provide a Pareto front (PF) with various non-dominated optimal solutions that balance competing goals. This research employs the SHADE, GWO, success-history based adaptive differential evolution-superiority of feasible solution (SHADE-SF), SF-MFO, and MFO algorithms to analyze five objective problems from the IEEE 57-bus benchmark. A complete list of abbreviations is listed in *Appendix I*. As shown in *Appendix II*, SF-MFO has a lower computational complexity than MFO and SHADE. By simply normalizing the objectives, SF-MFO can accommodate significantly different goals. The technique, however, was created for use in situations where several objectives could be pursued without any restrictions. Until now, SF-constraints MFOs have been managed via a penalty function technique. The choice of penalty coefficient affects this method. To establish the findings of the case scrutinized, a particular correct choice of penalty coefficient can cause a breakdown in the system's restrictions. Therefore, when employing the penalty function approach, care must be taken to choose just practical options. A good constraint handling (CH) method makes selecting a penalty coefficient easier. Together, the CH method and an appropriate evolutionary algorithm quickest explore the practicable approximately and aid in defining the border between the infeasible and durable zones.

3.5Cost estimation for overestimated or underestimated solar energy production

The histogram in *Figure 2* depicts the PV facility's attainable speculative energy. Here, the maximum accessible actual energy for this station is controlled at the appraised energy of the PV station (i.e. 50 MW). While the position has the probability of harvesting extra cosmic power than the plant's rated capacity, the PV station authority cannot be eligible to forfeit cost before the appraised size for that station. The magenta dashed line depicts the power the PV plant is expected to feed into the grid. As indicated earlier, the scheme energy might be a consignment of electricity unanimously agreed by ISO and the cosmic energy proprietor. When estimating the price of an overestimate, one can use the following formula (the subscript 'k' in Equation 9 is deleted for an isolated cosmic energy station):

$$C(P_{ss}-P_{sav})=K_{Rs}(P_{ss}-P_{sav}) \\ =K_{Rs}\sum[P_{ss}-P_{sn}]N_{b-n}=1*f_{sn} \quad (20)$$

where P_{sn} is the accessible energy below the scheme energy P_{ss}, and f_{sn} is the comparative oscillation of circumstance of P_{sn} on the first portion of the position of P_{ss} in the bar graph [43] for the stopcocks area consequence. The number of pairings (P_{sn}, f_{sn}) created for the PDF equals the aggregate of different case bins on the first portion side of P_{ss} or N_b. Here, average (P_{sn}, f_{sn}) values of the bins (segments) are considered in calculations to lessen the computational strain at each iteration. The results become more reliable as more segments are utilized. The findings of our analysis show that a total of 30 segments (N_b) are sufficient to solve the situation at hand.

3.6Power consumption forecasts versus prices (Breeze together with cosmic energy)

In this example, the Weibull PDF framework matches those within *Table 2*. Parameters that are important for a wind turbine to operate are listed in section 2.4. Wind energy's g_1 = 1.6 and g_2 = 1.75 direct cost coefficients are relatively low. It is assumed that the secondary price portion being exaggerated is $KR_{w,1}$ = $KR_{w,2}$ = 3 and the penalty mentioned above price coefficient for underutilization of full available wind power is $KP_{w,1}$ = $KP_{w,2}$ = 1.5. Remember that the forfeit price no longer utilizes available breeze energy that is below the control price of renewable energy, and both are below the standard price over scorching power [44]. *Figure 2* shows the reserve, penalty, direct, and total cost variations for the two wind farms as the scheduled energy found changed from zero to the estimated energy of the wind farms. By extension, the secondary generation cost rises as scheduled power rises for a greater rotating secondary is essential. The penalty fee falls with increasing scheduled power, as it should, albeit at a slower rate.

3.7Carbon tax enables the cheapest possible power generation

This scenario minimizes the carbon price levied on conventional thermal power plants' emissions. The goal is to diminish the combined price, which may be calculated using (6). Assume a carbon emissions Ctax of $20 per ton [45]. Because of the carbon price component, sustainable power, in particular breeze and cosmic energy, is predicted to expand in popularity. *Appendix III* displays computed parameters, including the optimal generating scheme, alternator receptive energy, combined production price (in addition to coal charge), and more. In Case 5 (with a carbon tax), it is seen that wind and solar energy penetration is more significant than in Situation 1 (without forfeit on emanation). The

excretion capacity with the estimated coal charge applied determines concerns about the escalation in optimal production from sustainable power.

3.8Algorithm for optimality with moth-flames

Based on the simulation of moth behaviour for their unique nighttime navigation techniques, Seyedali Mirjalili proposed MFO, a new metaheuristic optimization method, in 2015. They find their way around via a technique called transverse orientation. This highly systematic procedure exposed notable separation for the coherent rule, as the moon was out of the moth's sight for most of the flight. This system ensures that moths always take a direct route when flying at night. However, we often see moths circling the lights in a helical pattern. This sort of behaviour results from moths being deceived by artificial lighting. Moths' spiral flight paths [46] are caused by their attempts to keep a constant angle with the light source, which is the moon. In the MFO algorithm, moths circle a candle or light source in a logarithmic spiral before settling in on it. The optimal solution is guaranteed to be exploited, and the spiral path expresses the exploration region. Here, "optimization" describes all methods for locating the most desirable answers to issues. The necessity for novel optimization strategies has become increasingly clear in recent decades due to the growing complexity of problems. Before the advent of heuristic optimization methods, mathematical optimization techniques were the only available instruments for maximizing the efficiency of a given process. Most deterministic mathematical optimization approaches have a severe flaw: they get stuck in a never-ending cycle of finding and re-finding local optimums. Some of them, like the gradient-based technique, also need the search space to be derived. The optimal solution is guaranteed to be exploited, and the spiral path expresses the exploration region. Here, "optimization" describes all methods for locating the most desirable answers to issues. The necessity for novel optimization strategies has become increasingly clear in recent decades due to the growing complexity of problems. Before the advent of heuristic optimization methods, mathematical optimization techniques were the only available instruments for maximizing the efficiency of a given process. Most deterministic mathematical optimization approaches have a severe flaw: they get stuck in a never-ending cycle of finding and re-finding local optimums. Some of them, like the gradient-based technique, also need the search space to be derived.

3.9 SF-MFO and Wilcoxon test model design

Deterministic exploration (DE) begins by including community for erratically initiated successor suspension (Np vectors, each of d dimensions) naturally for explore duration determined for inferior and higher constrained, as shown in *Figure 4*. This j^{th} element based on i^{th} settlement direction is set to the following values before being seeded into the population Equation 21:

$$x(1) = x_{\min,j} + rand_{i,j}[0,1].(x_{\max} - x_{\min,j} \quad (21)$$

where $rand_{i,j}$ [0,1] indicates arbitrarily, the character bounded zero together with one, and the salutation '1' signifies actualization. wherever 'N_p' for community magnitude together with 'd' exits proportions for settlement angle, i=1,2,…,N_p also j=1,2,…,d.

Wilcoxon Test Model: The model is expressed as Equation22:

$$W = \sum_{i=1}^{N_r}[sgn\,(x_{2,i} - x_{1,i}) \times R_i] \quad (22)$$

W= test statistic

N_r=Sample size, excluding pair where $x_1=x_2$

Sgn=Sign Function

$x_{1,I}$, $x_{2,i}$= corresponding ranked pairs from two distributions

R_i= Rank i

3.10 Excellency for SF algorithms for creating realistic solutions

When comparing two solutions, SF [47] uses a pairwise comparison. When (x_i) is doable and (x_j) is not, solution (x_i) is preferred above (x_j). Both x_i and x_j are workable, but x_i minimizes the scheme service (for depreciation drawback) better. Both x_i and x_j fall impractical, yet x_i leads close to less severe contravention of the constraints on the whole (i.e., io (x_i) io(x_j) according to (21). Consequently, in this method, feasible persons are prioritized above infeasible ones. When comparing two solutions, one uses the objective function value to determine which is better, while the other uses the number of constraints violated to determine which is worse.

3.11 Combining CH methods with the SF-MFO algorithm

SHADE's and DE's selection procedure is unrestricted. When the SHADE innovation ensures use beside a CH approach, the choice for the creature of the following produce abides by the constraints of this CH technique. In *Figure 5*, a flowchart describing collaborative SHADE-XX (XX: SR/SF/EC) innovation is stated with an example. The flowchart furnishes an aristocratic view as concerned steps, while the worktable provides a comprehensive narrative strategy. It should be noticed that the algorithm loop's step 3 (selection step) varies

depending on the CH technique (in addition to CH method-specific parameters).

3.12 Techniques for addressing constraints

By imaginary creation for EAs impossible solutions should not be immediately rejected. When combined for a suitable EA, it is a cognate effective restriction handling technique that can direct hunt summons toward globally applicable culmination promoting for perception restrain up on the insurmountable result. Appropriate restriction operation for stable forfeit often adds forfeit suitability for impossible results because it violates all limitations. Resembling clarity and convenience for use, the consistent forfeit procedure efficacy should strongly be considered a punishment aspect that must be adjusted by proof and study.

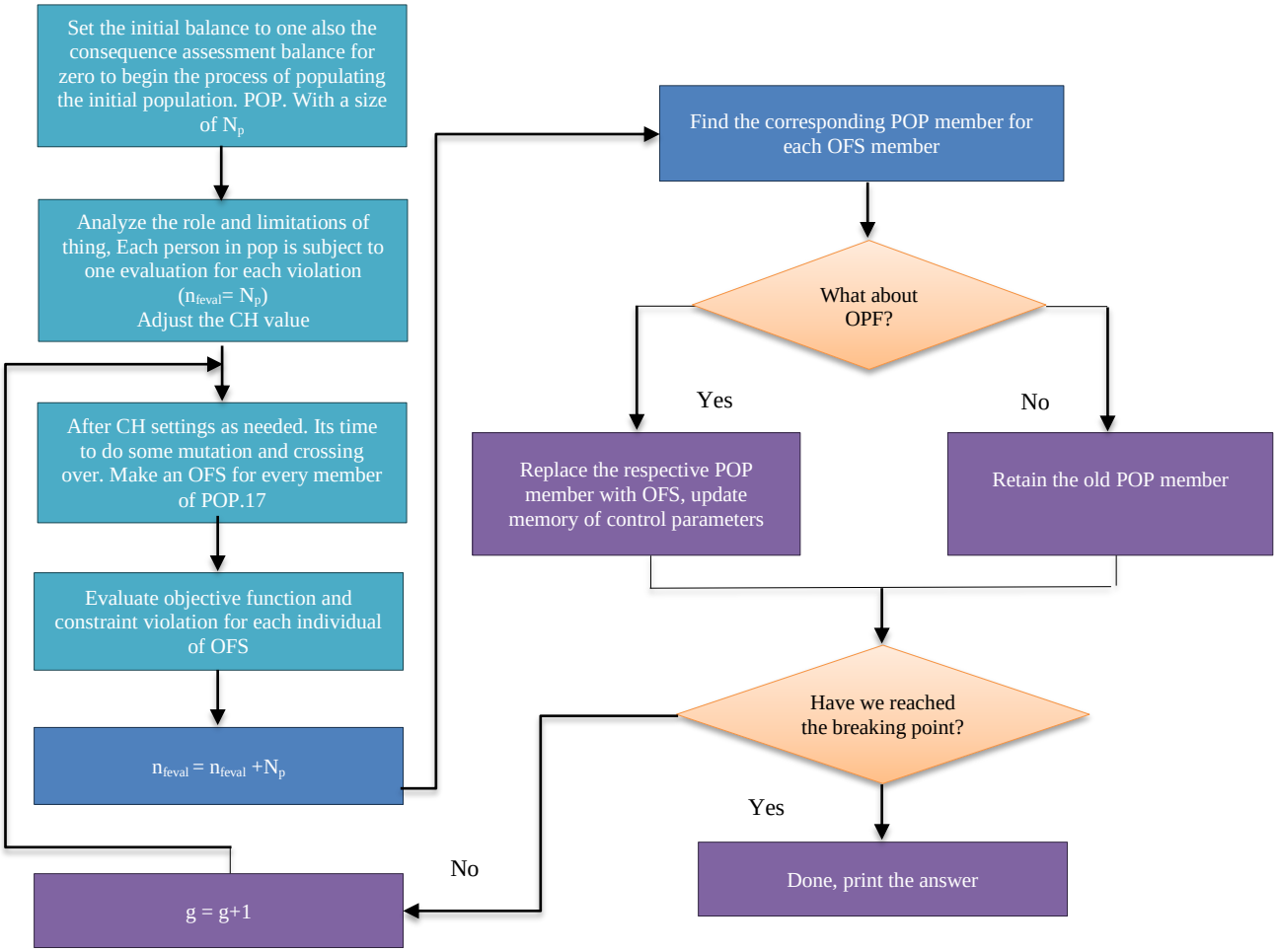

Figure 4 SF- MFO algorithms

Comprised of the subsequent stages is the SF-MFO algorithm:

Step one

•Initialize the Np population by employing a uniform random distribution.

•Input one (b) into the counter for generation. Determine the criterion for termination, which is the utmost number of generations (G).

Step two

•In order to generate new offspring, Ni individuals must undergo SF operations (mutation and crossover) by a predetermined scale factor (a) and CR (aa).

Binomial crossover is utilized when combined with the DE/rand/1 mutation strategy.

The sum of all constraint violations is calculated for each generation using Equation (21).

• Incorporate $2Ni$ individuals into the population as descendants of the initial members.

In the **third stage**, viable solutions are identified.

• Determine viable resolutions—those that adhere to established parameters. If the number of viable options is smaller than the population size (Np), proceed to Step 5.
•If the merged population contains at least p viable individuals, proceed to step 4.
Step 4: Selection and normalization.
•Utilize Equation (20) to determine the normalized objective value for each objective and solution.
• Calculate the Euclidean distances of the summated normalized objective values for the origin. The halting point refers to the solution whose total normalized objective value is closest to the origin. The fallback set comprises unselected solutions and those significantly impacted by the halting point.
Fifth phase-Termination
•During the termination phase, which occurs during the fifth phase, increment the generation counter by one ($b + 1$).
• Cease if the halting condition outlined in $iabmu$ is fulfilled. Otherwise, proceed to step 2.

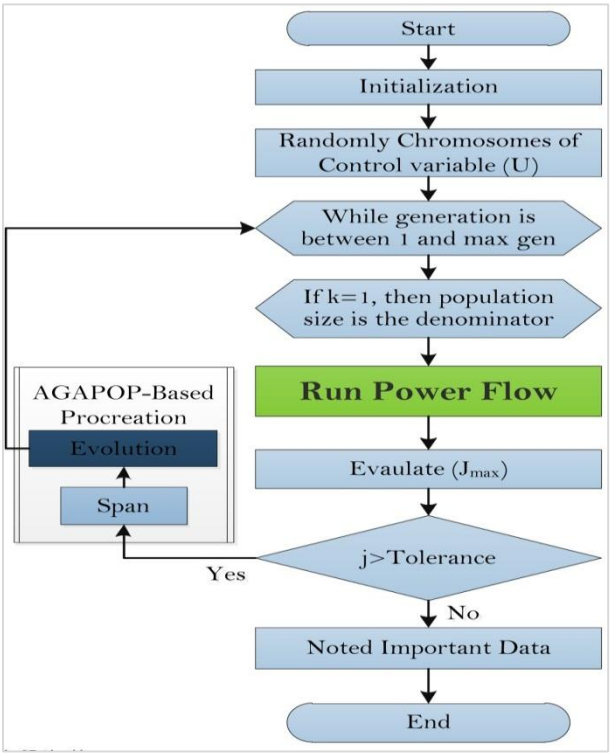

Figure 5 The SF algorithms

3.13Developed of grey wolf optimizer

A communal order of grey wolves inspired GWO [48], a powerful swarm-based optimizer [49]. In administration, grey wolf troops were split up toward quadrupled equalized alpha, beta, omega, and delta. Here, the pack's leader directs them, and the other wolves obey its commands since the alpha wolf (α) is at the top of the social hierarchy. For subsequent equality of leadership, the beta wolf (β) directly assists the alpha wolf in carrying out pack activities. Delta wolves(δ) are found on the third level of the hierarchy, below and above other wolves. The remaining wolves are the omegas (ω), always obligated to yield completely authoritative wolves. Here, the communal order of wolves is ranking of wolves in GWO [50]. The fittest solution in the GWO mathematical model is denoted by alpha, whereas beta and delta are the subsequent and tertiary results. Omega is the last of the possible solutions to be considered. The GWO, however, is dependent on tertiary dependent: A. Surrounding hunt. B. pursuing the quarry. C. Slapping the victim.

4.Results

This area includes sample research, replicate consequence results for applications of the SHADE-SF, SHADE, SF-MFO, MFO, GWO algorithms, and comprehensive system-by-system explanations and comparative assessments. The techniques are discussed, and *Table 3* provides a bit-by-bit process for resolving abstain maximization complications. The simulations for the suggested algorithms are tested on a machine along Intel® Core™ i7-106567 cpu@1.3 GHz. The algorithms were constructed using MATLAB software. *Appendix II* shows an adjustable increment constant such as the design indicates. *Appendix III* shows the scheme of several instant curricula conducted for analysis structure using every five designs compiled. The checkboxes in the table cells relate to the parameters that need to be optimized for a particular situation. Upon completion of 200 trials, the population sizes (PS) are chosen. The population's growing size badly affects the algorithm's ability to find workable solutions. For the IEEE 57-bus system, 32,000 function evaluations of objective functions are completed in one run. To do a demography investigation cognate assesses the effectiveness of the five coercion manipulation approaches, each example is run 30 times separately. The basic search algorithm was used to analyze 30 shuffles in each research instant (cases 1–5), employing various constraint-handling strategies. In a perspicuous procedure, no one can consistently deliver the best mean values or fitness. The Wilcoxon endorsed [51] method is utilized to evaluate how well each pair's innovation compares. SHADE-SF and SF-MFO are implemented accordingly for each instance, with the exception of cases 1, 4, and 5, where GWO is deemed superior. Except for example 4, SHADE-SF and GWO outperform SF-MFO. In scenario 4, all

algorithms perform similarly well. The performance comparison between SHADE-SF and SF-MFO raises an intriguing point. Although their performance is usually statistically comparable, no single method could consistently achieve the minimum best and minimum mean values. However, for larger systems with more decision factors, SF-MFO consistently outperforms SHADE-SF.

4.1Combustible charge optimization

In a typical combustible charge optimization scenario, algorithms such as SHADE-SF and SF-MFO yield fuel prices of $29,876.0856179 and $26,466.41033 per hour, respectively (*Table 3*). Relating to a productive total structural restriction and, more precisely, substantiating the top bounds for considerable discriminating restriction for production receptive energy, feeder line potential. *Table 3* presents the objective functions for the best, worst, average, and std dev results in each scenario.

Table 3 Generation cost minimization

Algorithms	Best results($/hr)	Worst	Average	Std Dev
GWO	29242.7429	33303.5121	31140.1479	829.39991
SHADE-SF	29876.0856	34512.5121	31238.7623	829.39991
SHADE	28563.0823	32642.5121	31007.4583	829.39991
MFO	31460.7087	33515.4683	31878.3296	531.96986
SF-MFO	**26466.4103**	30847.3470	29718.4417	1098.88723

The operational potential for capacity feeders is frequently initiated close to the limitations, making restriction for capacity feeder potential one of the essential inequality constraints. Better outcomes [52–55] than those achieved by the five methods in the current study were reported in several previous articles. A closer examination of that data reveals that the solutions are infeasible as they violate voltage limitations [0.97 p.u. - 1.05 p.u.]. According to potential profiles for the capacity feeder in *Figure 6*, here assumed a particular violation has most likely happened over the maximum limit. Overvoltage is bad since it can stress the system and frequently causes associated equipment to fail. The largest progressive aggregate for perfect voltage deviation (VD) in Equation 17 that might theoretically occur if all these buses function at their limitations mentioned 1.2 p.u. (or 240.05 p.u.). In many instances, the proclaimed estimate VD values for specific dissemination may be excessive compared to 1.2 p.u.

As it turns out, the static penalty method's problematic outcome is sensitive to alternative collegial forfeiture. The boxplot in *Figure 7* shows the resilience of the SF-MFO. Limitations for completely conversely vulnerable inconsistent are an excellent analytical solution for this specific OPF issue. The limitations on these variables are frequently broken in the static penalty function technique, possibly without the programmer's knowledge. The advantage of a proper CH technique also rests in its capacity to provide the optimal outcome while permitting operating close to the boundaries. The load bus convergence curve for the case studies carried out in IEEE 57- feeder structure is presented in *Figure 8*. The control variables for a case study determined using the strategy that performed best in that situation are provided in Appendix *II* and are the voltage profile for that case study.

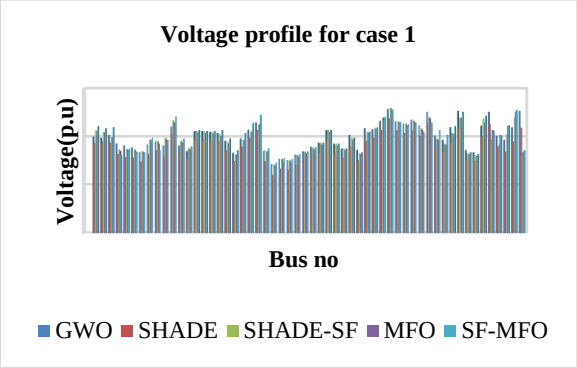

Figure 6 Voltage profile for case 1

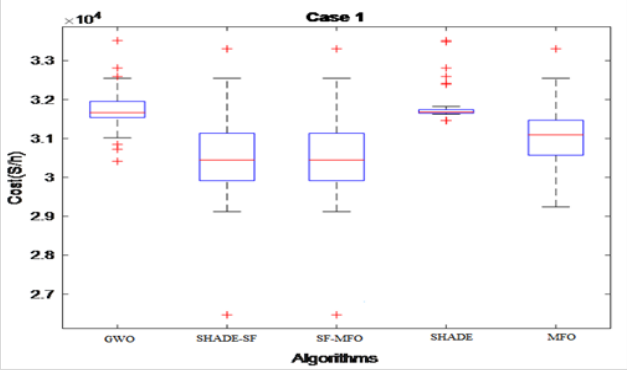

Figure 7 Boxplot for case 1

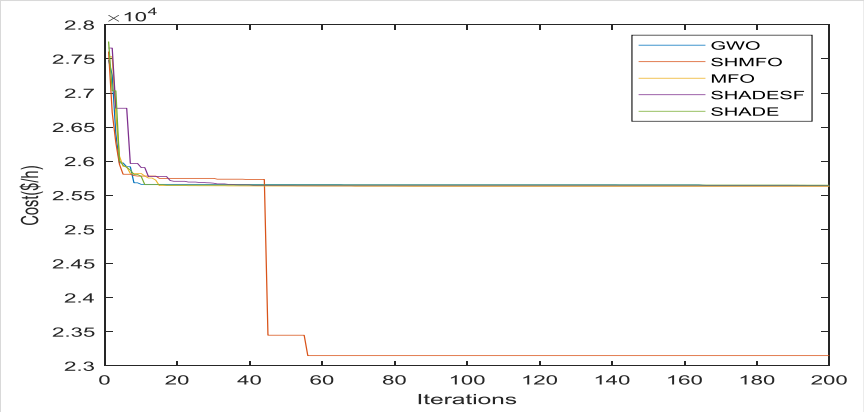

Figure 8 Convergence curve for case 1

4.2Minimizing actual power loss

This results in the SF-MFO algorithm's lowest value of 117.35601151 MW, obtained from *Table 4*. The fitness values discovered using the five methods are, on average, better than the vast majority of other values described in the compositions. The aptitude portrait of the capacity feeder in a perfect instant two experiments completed for the IEEE 57-feeder structure are shown as curves in *Figure 9*. All voltages are within acceptable ranges. In a few case studies, specific feeder potentials were discovered to be relatively adjacent to the maximum confine. This reality underlines the importance of exercising supplementary awareness when constructing potential constraints to prevent system bus overvoltage. The boxplot in *Figure 10* shows that SF-MFO is better than other algorithms. In *Figure 11*, merging slope, for instance, 2 using 3-CH approaches are stacked. It demonstrates a comparatively quick merging for a robustness estimate for SF-MFO and SHADE-SF. GWO seems to have converged more quickly than the other techniques. Subsequently, a fixed aggregate of consequence assessment, all curves are displayed. It is important to note that during the early stage of the exploration exercise, the design (CH method) searches for workable explanations. The actual convergence to the best solution begins when the search process enters the feasible zone.

Table 4 Minimizing of actual power loss

Algorithms	Best Results (MW)	Worst	Average	Std Dev
GWO	120.05246417	27.08358334	22.2172303	1.715989084
SHADE-SF	118.774974	21.783287	19.678238	1.715989084
SHADE	119.783471	23.797652	22.657197	1.715989084
MFO	119.68217772	22.94444462	20.1987465	0.801277302
SF-MFO	**117.35601151**	29.87107073	23.81237599	2.14365366

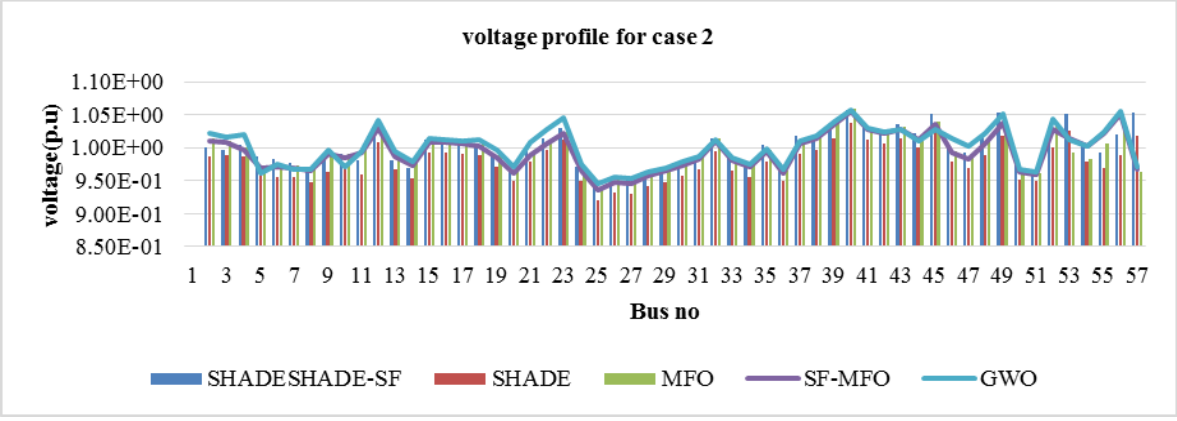

Figure 9 Voltage profile for case 2

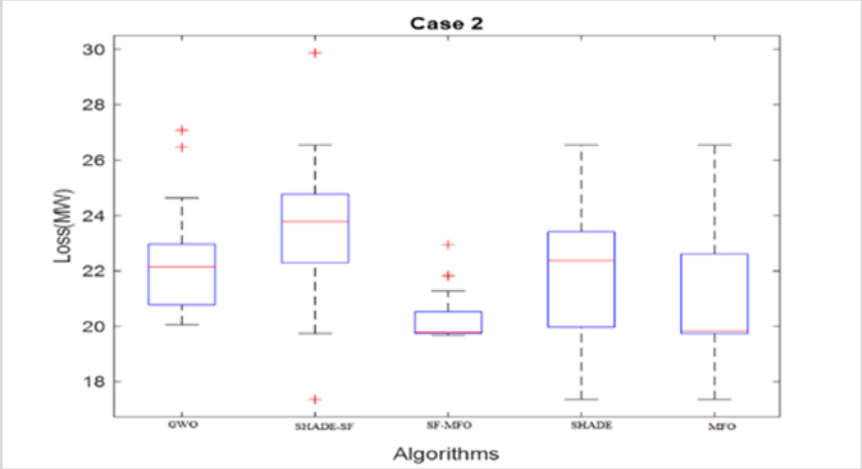

Figure 10 Boxplot, for instance, case 2

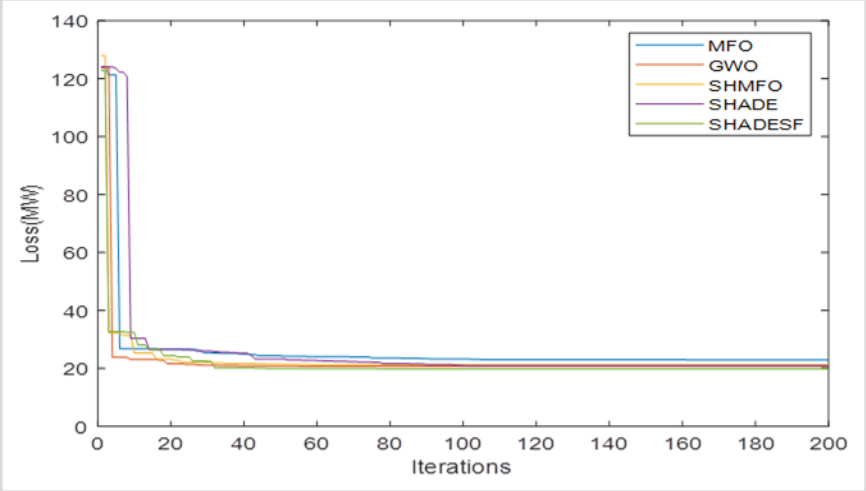

Figure 11 Convergence curve for case 2

4.3Instance 3- potential profile

The potential reliability index is decreased by 1.2402%, 1.5467%, 1.5432%, 1.5642%, and 1.5436% when considering the potential consistency implication as the objective function using the SF-MFO, MFO, SHADE, SHADE-SF, and GWO approaches, respectively. The convergence plot of the potential reliability implication for each technique is compared in *Table 5*. The findings indicate that reducing the voltage stability in the *Figure 12* index does not affect the loss value. Cost-based OPF methods are found to be inadequate for achieving loss minimization or voltage stability index goals. In the boxplot of *Figure 13*, SHADE-SF provides the lowest price, even though SF-MFO yields the lowest voltage stability index.

4.4Case 4: loss in exhalation

The exhalation converges the plot, boxplot, and potential portrait delineated in *Figure 14*, *Figure 15*, and *Figure 16*, which show the emission. The detailed results are shown in *Table 6*. The reduction percentages are as follows: MFO - 1.087%, SF-MFO - 0.909%, SHADE - 2.272%, SHADE-SF - 1.236%, and GWO - 1.364%. Enhancing this objective function would negatively affect the cost value. Compared to the base value, the cost value has increased by 2.46%, 2.13%, 8.46%, 3.46%, and 3.71%, respectively. Therefore, the objective function of minimizing emissions is best accomplished through SF-MFO.

Table 5 Voltage deviation

Algorithms	Best Results (p.u)	Worst	Average	Std Dev
GWO	1.5436	1.567	1.554	0.456
SHADE-SF	1.5642	1.5876	1.5785	0.5632
SHADE	1.5432	1.5543	1.5467	0.435
MFO	1.5467	1.6543	1.5576	0.5432
SF-MFO	**1.2402**	1.5651	1.3880	0.0648

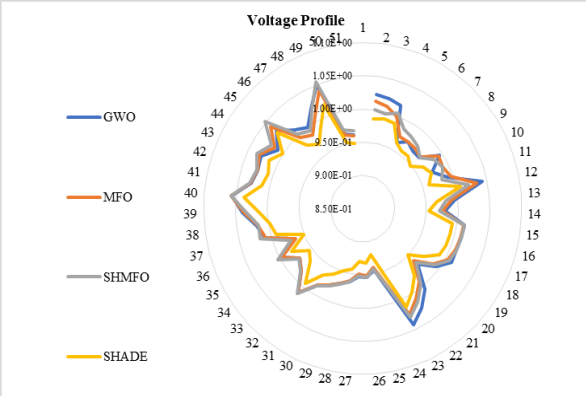

Figure 12 Voltage profile for case 3

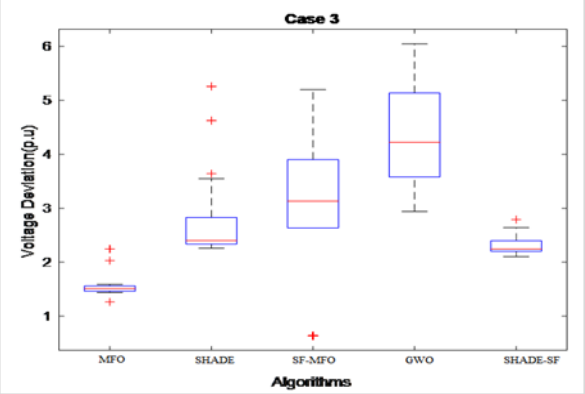

Figure 13 Boxplot for case 3

Table 6 Emission loss

Algorithms	Best Results	Worst	Average	Std Dev
GWO	3.764	5.87556	4.34566	0.7765
SHADE-SF	2.87654	3.9876	3.38765	0.78793
SHADE	3.76543	4.87654	4.24654	0.65712
MFO	3.12654	4.34512	3.998376	0.64521
SF-MFO	**1.98876**	2.9875392	1.998718	0.78612

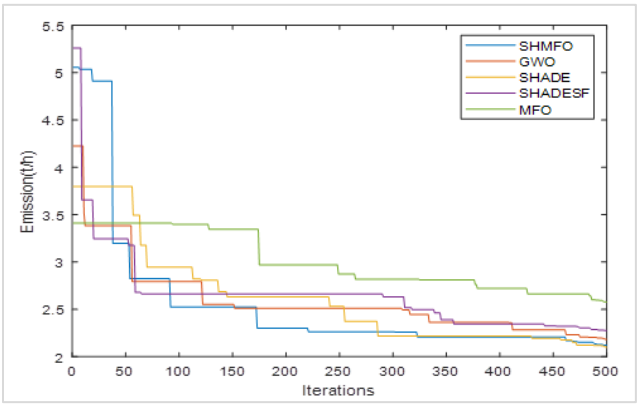

Figure 14 Case 4 coincides with the curve

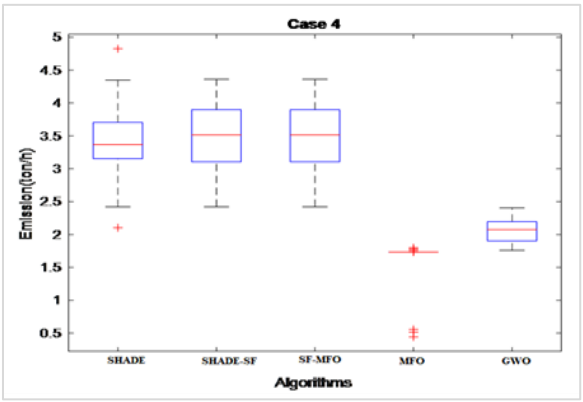

Figure 15 Boxplot for case 4

4.5Reducing expenses and carbon emissions

Table 7 presents cost-emission data that demonstrates the best middle ground soluions are 28129.41033, 29762.70873, 29762.0823821, 29672.0856179, and 29248.74294 $/h fuel cost with 1.98876, 3.12654,3.76543,2.87654, and 3.764 ton/hr emission for SF-MFO, MFO, SHADE, SHADE-SF, and GWO respectively. Therefore, SF-MFO presents lower prices and lower emissions.

The convergence curves do not represent the initial search phase fitness progression. Case 5 convergence curves are depicted in the *Figure 17*. The contrast outcome accomplished among SF-MFO and MFO is 1633.2984 $/h aforesaid $1633.2984/h × 8760 h = $ 14307694 price conservation year by year. Boxplot

for this scenario is provided in *Figure 18*, which displays the distribution of outcomes across all techniques for 30 iterations. This demonstrates that SF-MFO provides better accuracy than the competing algorithms. The SHADE-SF algorithm has very slow convergence and requires an enormous aggregate for consequence consideration to extend the best possible determination. This graph demonstrates that SF-MFO provides better accuracy than the competing algorithms.

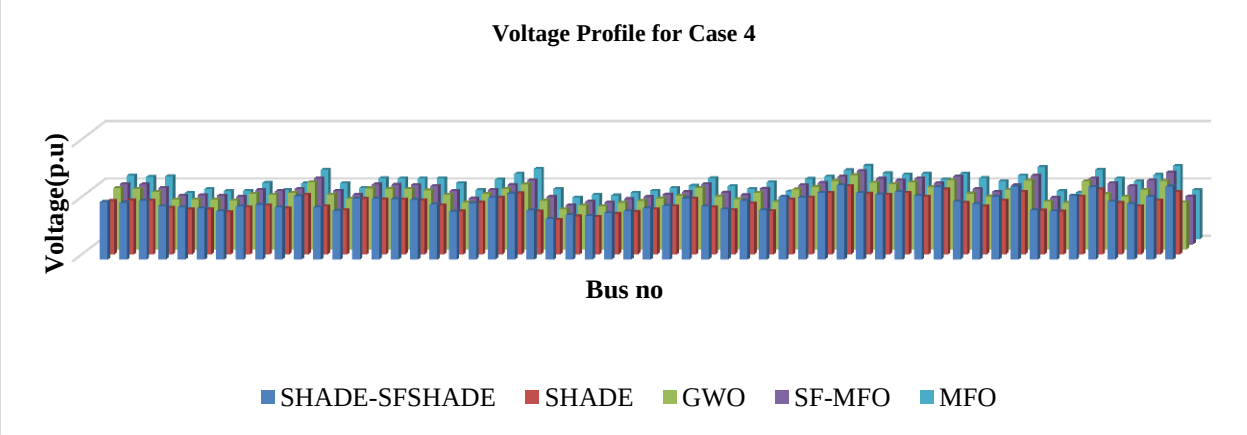

Figure 16 Voltage profile for case 4

Table 7 Total generation and emission cost

Algorithms	Best Results	Worst	Average	Std Dev
GWO	29248.74294	33127.51217	32140.14792	6559.38768
SHADE-SF	29672.085617	35512.51217	34238.76238	789.39197
SHADE	29762.082382	34762.51217	33007.4583	729.3999198
MFO	29762.70873	34987.46837	32878.32965	671.969876
SF-MFO	**28129.41033**	32987.34702	30718.44171	1378.45672

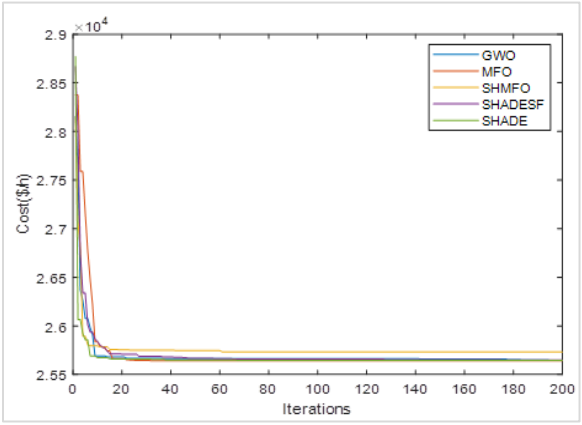

Figure 17 Merging slope of instance 5

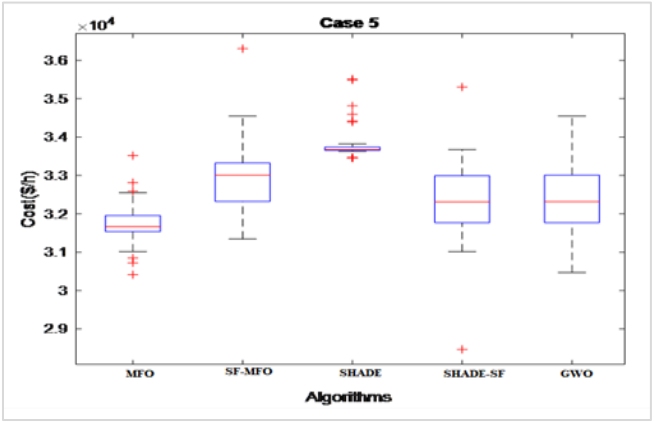

Figure 18 Boxplot for case 5

5.Discussion and limitations

The study introduces SF-MFO, an evolutionary-based metaheuristic algorithm, for solving the OPF problem across various objective functions including generation cost minimization, transmission loss minimization, VD emission minimization, and generation cost with emission effects. Results indicate SF-MFO's superior performance, achieving significant cost savings, loss minimization, and emission reductions compared to other algorithms. For instance, SF-MFO achieves significant cost savings, transmission loss minimization, and emission reductions for IEEE 57-bus systems. Specifically, it results in $26,466.4103/hr for power generation costs, 117.35601151 MW for transmission loss minimization, and 1.98876 tons/hour for

emission minimization. These figures translate to a remarkable 1.05%, 1.04%, and 1.3% cost saving per hour compared to the worst results obtained from other algorithms. When considering annual calculations, SF-MFO demonstrates substantial savings, with $1,3429.56 in cost savings, 2456.8 MW loss minimization, and 2654.2 tons emission reduction for IEEE 57-bus systems, respectively.SF-MFO's implementation in OPF, especially considering stochastic wind-solar-mini hydro power generators, marks a notable contribution. Comparative analyses highlight SF-MFO's effectiveness compared to existing metaheuristic algorithms in the OPF domain. Furthermore, the novelty lies in SF-MFO's application in OPF with stochastic renewable power generations, a facet previously unexplored in the literature.

The implications of SF-MFO's success extend to its potential as a viable solution for OPF problems, particularly in incorporating renewable energy sources into power system optimization. However, the longer computation time required by SF-MFO suggests a need for parallel computing implementation to alleviate computational burdens and enhance efficiency.

SF-MFO's computational complexity and longer computation times pose challenges, albeit mitigable through parallel computing strategies. Recommendations include further research on multi-objective metaheuristic algorithms for OPF problems and exploring avenues for reducing computational burdens through parallel computing. In comparative analysis, SF-MFO emerges as a promising solution for OPF problems, surpassing other algorithms in terms of cost savings, loss minimization, and emission reductions. Its application in incorporating stochastic renewable power generations signifies a significant advancement in OPF optimization techniques.

Limitations:
The presented data offer valuable insights into the performance of various optimization algorithms, such as SF-MFO, GWO, and SHADE, SHADE-SF and SF-MFO in solving different instances of the power system optimization problem. However, several limitations should be considered when interpreting these results. Firstly, the performance of the algorithms may vary depending on the specific characteristics and constraints of the power system under consideration, which may not be fully captured in the provided data. Additionally, the choice of objective functions and constraints may influence the comparative performance of the algorithms, potentially limiting the generalizability of the findings. Furthermore, the computation time required by each algorithm, as indicated in Appendix A1, could pose practical constraints, particularly for real-time or large-scale optimization problems. Moreover, the reported results may be sensitive to the parameter settings and tuning of each algorithm, which could affect their performance across different instances of the problem. Lastly, while the presented data offer valuable insights, further validation and analysis are necessary to fully understand the capabilities and limitations of each optimization algorithm in solving complex power system optimization problems.

6.Conclusion and future work

The research explores the feasibility and efficacy of the SF-MFO algorithm in addressing optimization challenges within power systems, particularly focusing on the IEEE 57-bus system for OPF. Through an in-depth analysis, the study discusses the integration of single- and multi-objective evolutionary techniques, highlighting the significance of utilizing a robust CH strategy in contrast to traditional penalty function methods. The SF-MFO algorithm is evaluated alongside other optimization methods, including SHADE, GWO, and MFO, showcasing its superior performance in optimizing power system operation under various constraints and objectives. Moreover, comparisons of CH methods highlight the significance of using a robust CH strategy over traditional penalty function methods, particularly in constrained issues like OPF. The research also explores the application of SF-MFO in multi-objective OPF (MOOPF) problems, revealing its potency in addressing complex optimization challenges, including uncertainties in energy sources and power system security constraints.

The findings indicate that SF-MFO outperforms traditional optimization methods like GWO and demonstrates rapid and consistent convergence, especially when compared to conventional GWO. The study suggests future directions in expanding research to incorporate sustainable production units and address load unpredictability using SF-MFO, highlighting its potential implications in enhancing the efficiency and reliability of power system operation and planning.

The research demonstrates the potential of SF-MFO in efficiently addressing complex power system optimization problems, offering rapid convergence

and stable performance compared to traditional optimization techniques. The study provides insights into the challenges and opportunities in power system optimization, emphasizing the need for further research to enhance computational efficiency, scalability, and adaptability of optimization algorithms in real-world power systems. Future work aims to extend the application of SF-MFO and explore its integration with other nature-inspired and EA to tackle multi-objective optimization challenges in power system operation and planning.

Acknowledgment

This research received no external funding. The authors would like to express their gratitude to Dr. Md. Asadur Rahman, Assistant Professor in the Department of Biomedical Engineering at MIST, Bangladesh, for his guidance and contributions to enhancing the quality of the manuscript.

Conflicts of interest

The authors have no conflicts of interest to declare.

Data availability

None.

Author's statement of contribution

Md. Shaoran Sayem, Md. Mahfuzur, and **Mohammad Khurshed Alam** carried out the investigation, writing and editing. **Mohd Herwan Sulaiman, Asma Ferdowsi**, and **Md. Foysal** conducted a comprehensive review and editing of the paper.

References

[1] Skolfield JK, Escobedo AR. Operations research in optimal power flow: a guide to recent and emerging methodologies and applications. European Journal of Operational Research. 2022; 300(2):387-404.

[2] Rong F, He L, Huang S, Lyu M, He C, Li X, et al. A split Bregman method solving optimal reactive power dispatch for a doubly-fed induction generator-based wind farm. Scientific Reports. 2022; 12(1):1-16.

[3] Montoya OD, Gil-González W, Garces A. Sequential quadratic programming models for solving the OPF problem in DC grids. Electric Power Systems Research. 2019; 169:18-23.

[4] Mhanna S, Mancarella P. An exact sequential linear programming algorithm for the optimal power flow problem. IEEE Transactions on Power Systems. 2021; 37(1):666-79.

[5] Dahab M, Zakaria E. Linear programming based optimal power flow. Sudan University 2017.

[6] Nerger A, Martins AC, Soler EM, Balbo AR, Nepomuceno L. A nonlinear multi-period hydrothermal optimal power flow model for hydropower systems. International Journal of Electrical Power & Energy Systems. 2024; 155:109585.

[7] Leon LM, Bretas AS, Rivera S. Quadratically constrained quadratic programming formulation of contingency constrained optimal power flow with photovoltaic generation. Energies. 2020; 13(13):1-21.

[8] Gallego PLA, López-lezama JM, Gómez CO. A mixed-integer linear programming model for the simultaneous optimal distribution network reconfiguration and optimal placement of distributed generation. Energies. 2022; 15(9):1-26.

[9] Bayat M, Koushki MM, Ghadimi AA, Tostado-véliz M, Jurado F. Comprehensive enhanced newton Raphson approach for power flow analysis in droop-controlled islanded AC microgrids. International Journal of Electrical Power & Energy Systems. 2022; 143:108493.

[10] Tu S, Wächter A, Wei E. A two-stage decomposition approach for AC optimal power flow. IEEE Transactions on Power Systems. 2020; 36(1):303-12.

[11] Sadat SA, Sahraei-ardakani M. Initializing successive linear programming solver for acopf using machine learning. In 52nd north American power symposium 2021 (pp. 1-6). IEEE.

[12] Khan NH, Jamal R, Ebeed M, Kamel S, Zeinoddini-meymand H, Zawbaa HM. Adopting scenario-based approach to solve optimal reactive power dispatch problem with integration of wind and solar energy using improved marine predator algorithm. Ain Shams Engineering Journal. 2022; 13(5):101726.

[13] Han Y, Wu D, Cheng J, Wang J, Lu Y, Kong X. Optimal design and analysis of lubricating oil system in marine nuclear power based on adaptive genetic algorithm. Progress in Nuclear Energy. 2023; 166:104937.

[14] Papazoglou G, Biskas P. Review and comparison of genetic algorithm and particle swarm optimization in the optimal power flow problem. Energies. 2023; 16(3):1-25.

[15] Korab R, Połomski M, Owczarek R. Application of particle swarm optimization for optimal setting of phase shifting transformers to minimize unscheduled active power flows. Applied Soft Computing. 2021; 105:107243.

[16] Hai T, Zhou J, Alazzawi AK, Muranaka K. Modelling and simulation of photovoltaic system using hybrid improved shuffled frog leaping algorithm-fuzzy controller under partial shaded condition. Simulation Modelling Practice and Theory. 2023; 122:102684.

[17] Biswas P, Suganthan P, Amaratunga G. Optimal power flow solutions using algorithm success history based adaptive differential evolution with linear population reduction. In international conference on systems, man, and cybernetics 2018 (pp. 249-54). IEEE.

[18] Shankar R, Ganesh N, Čep R, Narayanan RC, Pal S, Kalita K. Hybridized particle swarm-gravitational search algorithm for process optimization. Processes. 2022; 10(3):1-13.

[19] Hu J, Song Z, Tan Y, Tan M. Optimizing integrated energy systems using a hybrid approach blending grey

wolf optimization with local search heuristics. Journal of Energy Storage. 2024; 87:111384.
[20] Bhadoria A, Marwaha S. Moth flame optimizer-based solution approach for unit commitment and generation scheduling problem of electric power system. Journal of Computational Design and Engineering. 2020; 7(5):668-83.
[21] Mahmoodi M, RA SM, Blackhall L, Scott P. A comparison on power flow models for optimal power flow studies in integrated medium-low voltage unbalanced distribution systems. Sustainable Energy, Grids and Networks. 2024; 38:101339.
[22] Stogner D, Wang X. Analysis and control for wind energy conversion system with five-level neutral-point clamped inverter. IFAC-PapersOnLine. 2023; 56(2):428-34.
[23] Yi T, Zhang C. Scheduling optimization of a wind power-containing power system considering the integrated and flexible carbon capture power plant and P2G equipment under demand response and reward and punishment ladder-type carbon trading. International Journal of Greenhouse Gas Control. 2023; 128:103955.
[24] Al-majali BH, Zobaa AF. A novel optimal allocation of STATCOM to enhance voltage stability in power networks. Ain Shams Engineering Journal. 2024:102658.
[25] De MI, Klymenko OV, Short M. Balancing accuracy and complexity in optimisation models of distributed energy systems and microgrids with optimal power flow: a review. Sustainable Energy Technologies and Assessments. 2022; 52:102066.
[26] Pattnaik A, Dauda AK, Padhee S, Panda S, Panda A. Security constrained optimal power flow solution of hybrid storage integrated cleaner power systems. Applied Thermal Engineering. 2023; 232:121058.
[27] Wang J, Song Y, Hill DJ, Hou Y. Preventive–corrective stability constrained OPF in microgrids for accommodating DG plug-and-play. International Journal of Electrical Power & Energy Systems. 2024; 155:109646.
[28] Bechlenberg A, Wei Y, Jayawardhana B, Vakis AI. Analysing the influence of power take-off adaptability on the power extraction of dense wave energy converter arrays. Renewable Energy. 2023; 211:1-12.
[29] Sulaiman MH, Mustaffa Z. Hyper-heuristic strategies for optimal power flow problem with FACTS devices allocation in wind power integrated system. Results in Control and Optimization. 2024; 14:100373.
[30] Yuan W, Sun Y, Su C, Wu Y, Guo H, Tang Y. Day-ahead optimal scheduling of hydropower-dominated power grids under a spot market environment. Journal of Cleaner Production. 2024:141350.
[31] Ramesh S, Verdú E, Karunanithi K, Raja SP. An optimal power flow solution to deregulated electricity power market using meta-heuristic algorithms considering load congestion environment. Electric Power Systems Research. 2023; 214:108867.
[32] Dora BK, Bhat S, Halder S, Srivastava I. A solution to multi objective stochastic optimal power flow problem using mutualism and elite strategy based pelican optimization algorithm. Applied Soft Computing. 2024; 158:111548.
[33] Bayat A, Bagheri A, Navesi RB. A real-time PMU-based optimal operation strategy for active and reactive power sources in smart distribution systems. Electric Power Systems Research. 2023; 225:109842.
[34] Yang H, Xu S, Gao W, Wang Y, Li Y, Wei X. Mitigating long-term financial risk for large customers via a hybrid procurement strategy considering power purchase agreements. Energy. 2024; 295:131038.
[35] Liu X, Huang T, Qiu H, Li Y, Lin X, Shi J. Optimal aggregation of a virtual power plant based on a distribution-level market with the participation of bounded rational agents. Applied Energy. 2024; 364:123196.
[36] Hussain R, Sabir A, Lee DY, Zaidi SF, Pedro A, Abbas MS, et al. Conversational AI-based VR system to improve construction safety training of migrant workers. Automation in Construction. 2024; 160:105315.
[37] Lambert A. A tight compact quadratically constrained convex relaxation of the optimal power flow problem. Computers & Operations Research. 2024; 166:106626.
[38] Rao AK, Kundu P. System integrity protection scheme for minimizing wind curtailment considering transmission line thermal limits. Sustainable Energy, Grids and Networks. 2023; 33:100970.
[39] Rafiee A, Karimi M, Safari A, Abbasi TF. The future impact of carbon tax on electricity flow between Great Britain and its neighbors until 2030. Applied Sciences. 2021; 11(21):1-15.
[40] Huang X, Kim JS, Hong KR, Kim NH. How do carbon trading price and carbon tax rate affect power project portfolio investment and carbon emission: an analysis based on uncertainty theory. Journal of Environmental Management. 2023; 345:118768.
[41] https://alroomi.org/power-flow/300-bus-system. Accessed 11 February 2021.
[42] Alencar MV, Da SDN, Nepomuceno L, Martins AC, Balbo AR, Soler EM. Discrete optimal power flow with prohibited zones, multiple-fuel options, and practical operational rules for control devices. Applied Energy. 2024; 358:122545.
[43] Ali A, Hassan A, Keerio MU, Mugheri NH, Abbas G, Hatatah M, et al. A novel solution to optimal power flow problems using composite differential evolution integrating effective constrained handling techniques. Scientific Reports. 2024; 14(1):1-27.
[44] Bideris-davos AA, Vovos PN. Co-optimization of power and water distribution systems for simultaneous hydropower generation and water pressure regulation. Energy Reports. 2024; 11:3135-48.
[45] Fu Y, Huang G, Xie Y, Liao R, Yin J. Planning electric power system under carbon-price mechanism considering multiple uncertainties–a case study of Tianjin. Journal of Environmental Management. 2020; 269:110721.

[46] Taher MA, Kamel S, Jurado F, Ebeed M. An improved moth-flame optimization algorithm for solving optimal power flow problem. International Transactions on Electrical Energy Systems. 2019; 29(3):e2743.
[47] Biswas PP, Suganthan PN, Mallipeddi R, Amaratunga GA. Optimal power flow solutions using differential evolution algorithm integrated with effective constraint handling techniques. Engineering Applications of Artificial Intelligence. 2018; 68:81-100.
[48] Yadav S, Kumar P, Kumar A. Grey wolf optimization based optimal isolated microgrid with battery and pumped hydro as double storage to limit excess energy. Journal of Energy Storage. 2023; 74:109440.
[49] Liu C, Li Q, Wei L, Li C. Wind power system based state estimation and measurement using weighted grey wolf optimization. Computers and Electrical Engineering. 2023; 110:108797.
[50] Yujie G, Hao Y, Bowen Z, Xinyi C, Zhijun H. Optimal operation of new coastal power systems with seawater desalination based on grey wolf optimization. Energy Reports. 2023; 9:391-402.
[51] Tian Y, Shi Z, Zhang Y, Zhang L, Zhang H, Zhang X. Solving optimal power flow problems via a constrained many-objective co-evolutionary algorithm. Frontiers in Energy Research. 2023; 11:1293193.
[52] Yu X, Wang H, Lu Y. An adaptive ranking moth flame optimizer for feature selection. Mathematics and Computers in Simulation. 2024; 219:164-84.
[53] Li C, Kies A, Zhou K, Schlott M, El SO, Bilousova M, et al. Optimal power flow in a highly renewable power system based on attention neural networks. Applied Energy. 2024; 359:122779.
[54] Jahed YG, Mousavi SY, Golestan S. Optimal sizing and siting of distributed generation systems incorporating reactive power tariffs via water flow optimization. Electric Power Systems Research. 2024; 231:110278.
[55] Chakraborty A, Ray S. Optimal allocation of distribution generation sources with sustainable energy management in radial distribution networks using metaheuristic algorithm. Computers and Electrical Engineering. 2024; 116:109142.

Mohammad Khurshed Alam, (L), BN (Retired) enlisted in the Bangladesh Navy on July 14, 1987, and was commissioned into the Electrical branch on January 1, 1990. He earned his degree in Electrical & Electronics Engineering from the Bangladesh University of Engineering & Technology (BUET) in 1993. In 1998, he traveled to England and Germany for PAXMAN Engine Operation and Maintenance Training. From 2002 to 2003, he completed the Navy Missile Maintenance Course in PRC. He also served as a contingent member in the UN Mission in Côte d'Ivoire from 2006 to 2007 and as a military observer in the DRC and CAR from 2013 to 2014. In 2013, he received a master's degree in Electrical and Electronics Engineering from Khulna University of Engineering and Technology (KUET), Bangladesh. Retired as a Lieutenant Commander, Alam held the position of Weapons Electrical Officer on the frigate BNS OSMAN and served in various capacities including electrical officer, engineer officer, and missile officer on different vessels. Currently, he is pursuing a doctoral degree at UMP in Malaysia and has been serving as an Assistant Professor of Electrical Engineering at AIUB in Dhaka since September 2019.
Email: PES20002@student.umpsa.edu.my

Mohd Herwan Sulaiman received his B. Eng. (Hons) in Electrical-Electronics, M. Eng. (Electrical-Power), and Ph.D. in Electrical Engineering from Universiti Teknologi Malaysia (UTM) in 2002, 2007, and 2011 respectively. Currently, he holds the position of Associate Professor at the Faculty of Electrical & Electronics Engineering, Universiti Malaysia Pahang (UMP). His research interests include power system optimization and the application of swarm intelligence to power system studies. He is one of the primary inventors of the Barnacles Mating Optimizer (BMO), a novel optimization algorithm inspired by nature. He is also an IEEE Senior Member. Enjoy writing and riding. He is now a runner as well.
Email: herwan@umpsa.edu.my

Md. Shaoran Sayem has completed his academic and professional journey in the field of Electrical and Electronic Engineering. Currently, he holds the position of a Lecturer (Sessional Faculty) at American International University-Bangladesh (AIUB), where he imparts his extensive experience gained from his previous role as a Network Engineer at LM Ericsson Bangladesh Ltd.(Department: Data Team). He also worked at Banglalink Digital Communication Ltd. as an intern (Department: Service Assurance Management, Active with Radio Team, Core Team, Troubleshooting, Report making, swap report, BTS visit). Md. Shaoran is a proud alumnus of AIUB, having earned both a Bachelor's and a Master's degree with prestigious "Megna-Cum-Laude" honors for his exceptional academic performance. His research interests and publications show his expertise in renewable energy and power systems. Md. Shaoran has not only achieved great success in his professional endeavors but has also made significant scholarly contributions, including a remarkable collection of conference papers and journal publications. His remarkable academic achievements have been acknowledged with accolades such as mentions on the Dean's Honor List. In addition to his academic pursuits, Md. Shaoran has actively contributed to industry projects, showcasing his practical skills and knowledge. Driven by his passion for advancing

sustainable technologies, Md. Shaoran continues to make significant contributions to the field. By combining his academic insights with practical experience, he strives to foster innovation and drive progress in the industry.
Email: shaoranmss@aiub.edu

Asma Ferdowsi earned her MBBS degree from Sher-E-Bangla Medical College in Barisal, which is affiliated with Dhaka University. Additionally, she received her MPhil in Pharmacology in 2022 from Sir Salimullah Medical College in Mitford, Dhaka 1100, and Bangladesh. Currently, he works as a lecturer at the same college. Her research into Renewable Energy Systems primarily concerns bio and medical refuse.
Email: asmaferdowsi7@gmail.com

Md. Foysal received his B.Sc. in Electrical and Electronic Engineering from American International University-Bangladesh (AIUB) in January 2023. Following his graduation, he interned with the Gazipur Palli Bidyut Samity under the Bangladesh Rural Electrification Board, serving as an Asset General Manager. He is currently pursuing an M.Sc. in Electrical and Electronic Engineering and is actively engaged in a research project focused on power systems. His research interests span a range of topics, including renewable energy systems, microgrids and hybrid power systems, wireless power transmission, and power system stability and control.
Email: mdfoysal571214@gmail.com

Md. Mahfuzur Akter Ringku received his B.Sc. in Electrical and Electronic Engineering from American International University-Bangladesh (AIUB) in January 2023. Following his graduation, he interned with the Gazipur Palli Bidyut Samity as an Asset General Manager under the Bangladesh Rural Electrification Board. He is currently enrolled in the Executive Master of Business Administration (EMBA) program, specializing in Accounting and Information Systems at the University of Dhaka. Additionally, he is working on a power system research project. His research interests include renewable energy systems (particularly wind and photovoltaic systems), the analysis and control of rotating electrical machines, microgrid and hybrid power systems, HVDC systems, and power system stability and control.
Email: mahfuzurakter@gmail.com

Appendix I

S. No.	Abbreviation	Description
1	CH	Constant Handling
2	CR	Crossover Rate
3	DE	Deterministic Exploration
4	DM	Decomposition Method
5	GA	Genetic Algorithm
6	ED	Economic Dispatch
7	EP	Evolutionary Programming
8	FSLPA	Fast Successive Linear Programming Algorithm
9	EA	Evolutionary Algorithms
10	FOZ	Forbidden Operating Zones.
11	F	Scaling Factor
12	GWO	Grey Wolf Optimization
13	GSA	Gravitational Search Algorithm
14	ISO	Independent System Operators
15	IP	Integer Programming
16	LP	Linear Programming
17	MFO	Moth Flame Optimization
18	MOOPF	Multi-objective OPF
19	MSFLA	Modified Shuffled Frog Leaping Algorithm
20	NM	Newton Methods
21	NLP	Nonlinear Programming
22	ORPD	Optimal Reactive Power Dispatch
23	OPF	Optimal Power Flow
24	PS	Population Sizes
25	PSHG	Pumped-Storage Hydro Generators
26	PDFs	Probability Density Functions
27	PF	Pareto Front
28	Np	Population Size
29	PV	Photovoltaic
30	PSO	Particle Swarm Optimization
31	QP	Quadratic Programming
32	SLP	Simplex-Based Sequential Linear Programming
33	SHU	Solar Hydro Unit
34	SQP	Sequential Quadratic Programming
35	SC	Shunt Capacitor
36	SF-MFO	Superiority of Feasible Solution-Moth Flame Optimization
37	SHADE	Success-History Based Adaptive Differential Evolution
38	SHADE-SF	Success-History Based Adaptive Differential Evolution -Superiority of Feasible Solution
39	VD	Voltage Deviation

Appendix II (Different Events 1–5 Detail Results)

	Restrict		Event 1				Event 2			Event 3			Event 4			Event 5		
ITEM	MIN	MAX	MFO	GWO	SHADE	MFO	GWO	SHADE	MFO	GWO	SHADE	MFO	GWO	SHADE	MFO	GWO	SHADE
Pg2	0.00	115.00	56.3	65.3	65.3	65.8	67.4	67.4	56.4	83.2	98	76.8	56.8	64	32.7	44.6	21.4
Pg5	0.00	140.00	54	67	65	57	74	55	53	67	54	56	76	87	98	87	78
Pg8	0.00	100.00	45	67	76	67	65	74	76	67	65	54	76	90	89	87	76
Pg11	0.00	550.00	43	54	56	87	76	76	46	87	67	77	87	67	76	67	78
Pg13	0.00	200.0	65	77	78	67	87	87	94	87	78	89	98	104	110	89	87

		0															
		210.0	72	75	86	76	72	77	67	76	67	82	75	87	79	88	95
Vg1	0.00	0															
Vg2	0.97	1.05	.90	.99	.99	.98	1.01	1.01	.99	.98	1.01	1.01	1.01	.99	1.02	1.01	.98
Vg5	0.97	1.05	1.05	.90	.99	1.01	1.01	1.02	.98	.99	.99	1.01	1.01	1.03	1.01	1.01	1.01
Vg8	0.97	1.05	.97	.98	.99	.98	.98	1.01	1.01	1.01	.99	1.01	1.01	1.02	.99	1.02	.99
Vg11	0.97	1.05	.99	.98	.98	.99	.99	1.03	1.02	1.01	.99	.98	.99	.99	.98	1.01	.99
Vg12	0.97	1.05	.97	.99	1.01	.99	1.01	1.01	1.01	1.01	.98	.98	.99	.99	.98	1.01	1.01
Vg13	0.97	1.05	1.01	.98	1.03	.99	1.02	1.02	1.01	1.02	1.01	1.02	1.01	1.01	1.01	1.01	1.02
$T_{6,9}$	0.95	1.05	1.02	1.01	1.03	.99	1.01	.98	1.01	.99	1.01	.99	1.01	1.03	1.01	1.01	1.02
$T_{6,10}$	0.95	1.05	1.01	.98	1.03	1.01	.99	.99	1.01	1.01	1.01	.98	1.01	1.01	.98	1.01	1.01
$T_{4,12}$	0.95	1.05	1.03	1.01	1.01	.99	1.03	.98	1.02	1.01	1.01	.99	1.01	1.01	1.01	1.01	1.01
$T_{28,27}$	0.95	1.05	1.01	.97	.98	1.3	.98	1.2	1.01	.99	1.02	1.01	.98	.97	.99	1.01	1.01
Q_{c10}	1	6	6	0	1	6	1	6	1	6	1	6	1	6	1	6	1
Q_{c12}	1	6	1	6	0	6	6	2	1	6	1	6	1	0	6	2	1
Q_{c15}	1	6	1	6	4	5	6	3	6	4	6	5	1	0	5	4	1
Q_{c17}	1	6	1	4	2	3	6	4	4	6	4	4	4	0	6	4	4
Q_{c20}	1	6	1	5	2	6	4	6	6	4	6	5	6	0	5	6	6
Q_{c21}	1	6	1	6	1	6	1	6	6	1	6	1	6	1	6	1	6
Q_{c23}	1	6	6	5	2	5	3	5	5	3	5	4	5	4	5	6	2
Q_{c24}	1	6	6	5	3	4	6	5	6	6	6	5	6	4	3	4	6
Q_{c29}	1	6	6	5	3	5	5	6	6	4	3	4	5	3	6	4	3
Fuel Cost($/h)		Valve	30010.5	30111.7	30212.6	30213.7	30050.6	30510.4	30060.7	30210.8	30010.7	30410.9	30510.4	30111.5	30612.7	30611.7	30815.8
Q_{gen}($/h)			118.1	122.3	121.4	119.3	214.3	213.4	213.2	246.3	267.2	254.1	245.1	244.2	245.1	264.1	246.1
$W_{gencost}$($/h)			234.8	237.4	243.4	245.5	265.4	265.4	265.6	277.4	267.3	261.6	276.4	265.3	287.8	256.4	276.3
P_{loss}(MW)			23	18	21	22	23	23	24	26	22	27	28	24	8	22	23
$G_{bestvalur}$($/h)			1782.5	1784	1786	1787.6	1837	1784	1784.6	1757	1765	1762.6	1794	1796	1774.6	1785	787
$F_{Emission}$(ton/h)			2.8	2.5	2.6	2.7	2.8	2.3	2.7	2.9	2.8	2.6	2.7	2.9	2.7	2.9	2.6
Computation time(s)			183.7	168.5	178.4	187.6	189.6	184.4	186.6	197.6	168.4	176.6	178.6	186.4	187.4	175.6	165.4

Appendix III

State variables	**Restrict**		**Case1**		**Limit**	**Case 2**		
	Min	Max	SF-MFO	GWO	Min	Max	SF-MFO	GWO
Pg1	55	210	55.342 MW	55.43 MW	-15	460	378.54 MW	378.345 MW
Qg1(Mvar)	-10	170.0	-25.00000	-25.00000	-150	210	29.6543	78.4532
Qg2(Mvar)	-10	65.0	22.6543	19.5643	-18	55	55.00000	55.00000
Qg5(Mvar)	-20	40.0	20.6543	22.456	-16	65	48.5613	-1.7654
Qg8(Mvar)	-20	50.0	45.00000	45.00000	-9	30	13.5643	20.00000
Qg11(Mvar)	-20	40.0	35.00000	31.543	-150	210	55.4567	55.6543
Qg13(Mvar)	-25	30.0	19.435	22.435	-5	10	8.00000	8.00000